Networks and Heterogeneous Media

https://www.aimspress.com/journal/nhm

NHM, 21(4): 1376–1392.
DOI: 10.3934/nhm.2026052
Received: 24 May 2026
Revised: 20 June 2026
Accepted: 30 June 2026
Published: 03 July 2026

Research article

Exact analytical results on synchronizability in multilayer networks

Jing Chen[1], **Dedian Li**[2], **Weigang Sun**[2,*] **and Xinke Zhao**[2]

[1] School of Information Technology, Zhejiang Yuying College of Vocational Technology, Hangzhou 310018, China

[2] School of Sciences, Hangzhou Dianzi University, Hangzhou 310018, China

* **Correspondence:** Email: wgsun@hdu.edu.cn; Tel: +8657186873881.

Abstract: Synchronization in multilayer networks plays a fundamental role in many real-world systems; yet, understanding how interlayer structures influence synchronizability remains a major challenge. In this paper, we investigated the synchronizability of multilayer networks with undirected and directed interlayer couplings. By deriving the exact spectral properties of the corresponding supra-Laplacian matrices, explicit synchronizability criteria were established for bounded and unbounded synchronization regions. The results revealed that interlayer coupling patterns strongly affected synchronization behavior. In undirected multilayer networks, increasing the number of layers weakened synchronizability, whereas stronger intra- and interlayer coupling strengths could enhance synchronization performance. In contrast, multilayer networks with directed interlayer couplings exhibited different behavior: Synchronizability became independent of the number of layers, demonstrating the significant impact of coupling asymmetry on collective dynamics. Moreover, simulations on Erdös–Rényi multilayer networks validated the theoretical predictions. These findings provide analytical insights into how multilayer architectures and coupling asymmetry shape synchronization dynamics and may offer guidance for the design and optimization of complex interconnected systems.

Keywords: multilayer networks; synchronization; synchronizability; Laplacian; supra-Laplacian matrix

1. Introduction

Complex networks [1, 2] provide a unifying mathematical paradigm for modeling and analyzing large-scale interconnected systems across research domains [3–6]. By abstracting individual entities as nodes and their interactions as edges, network science enables the quantitative characterization of structural organization and dynamical processes through rigorous graph-theoretic and spectral metrics.

Among collective dynamical behaviors, synchronization has emerged as a central topic in complex networks [7]. This phenomenon plays a crucial role in a wide range of real-world applications, including the design of resilient communication systems, the optimization of traffic and transportation networks, and the development of decentralized algorithms for distributed computing [8–10]. The emergence and stability of synchronization are determined not only by the intrinsic dynamics of individual nodes but also by the structural properties of the underlying network topology [11, 12]. When network synchronization cannot be achieved, control strategies, such as impulsive control, adaptive control, and pinning control, have been proposed to realize synchronization [13, 14].

The synchronizability of a network [15–17] describes its inherent ability to support and maintain synchronization behavior among interconnected nodes despite possible heterogeneity in node dynamics and network structure. It is closely related to the interplay between dynamical processes on the nodes and the structural properties of the network, and is characterized by spectral measures of the Laplacian matrix [18–20], which capture the effects of connectivity patterns and coupling strengths on collective dynamics. For networks with an unbounded synchronization region, synchronizability is governed by the second-smallest eigenvalue of the Laplacian matrix [21]. In contrast, for networks with a bounded synchronization region, synchronizability is determined by the eigenratio, defined as the ratio of the largest Laplacian eigenvalue to the second-smallest one [22]. In a single layer network, synchronizability is determined solely by the spectral properties of the corresponding Laplacian matrix. In contrast, a multilayer network involves intralayer and interlayer couplings, and its synchronizability is governed by the spectral properties of the associated supra-Laplacian matrix [23].

The spectral properties of multilayer networks have attracted considerable attention because they provide a fundamental framework for understanding synchronization, diffusion, controllability, and robustness in interconnected systems. In multilayer networks, the supra-Laplacian matrix plays a central role by integrating intralayer and interlayer coupling structures into a unified spectral representation. Early studies established the theoretical foundations for the spectral analysis of multilayer networks and demonstrated how interlayer couplings influence eigenvalue distributions and collective dynamics [24, 25]. Moreover, increasing attention has been given to the role of higher-order interactions and multilayer structures in shaping complex spatiotemporal behaviors. Representative studies include investigations of chimera states characterized by the coexistence of synchronized and desynchronized dynamics [26], synchronization conditions for chaotic systems in stochastic delayed multilayer networks with additive coupling [27], and unified theoretical frameworks incorporating higher-order interactions beyond pairwise couplings within and across layers [28].

Despite the expanded modeling capability of multilayer networks [29], analyzing and optimizing their synchronizability remains challenging. The primary difficulty arises from the intricate interplay between intralayer and interlayer coupling structures, which introduces multiple interaction scales and enlarges the dimensionality of the system [30–33]. Moreover, the structural complexity of multilayer networks makes it difficult to obtain explicit eigenvalues of the associated supra-Laplacian matrix. For example, Zhang et al. derived closed-form expressions for the eigenvalues of multiplex k-nearest-neighbor coupled networks [34], thereby showing the impact of structural parameters on synchronizability. Xu et al. investigated twolayer star networks and demonstrated how an increasing number of layers influences synchronizability [35]. Li et al. studied dumbbell-shaped networks and compared the effects of different inter-layer coupling configurations [36]. Moreover, Hu et al. developed a rigorous mathematical framework for determining the optimal interlayer edge configurations that maximize synchronizability in twolayer chain networks [37].

Motivated by the above discussion, we consider general intralayer network structures and derive exact synchronizability criteria in terms of the eigenvalues of the supra-Laplacian matrix for multilayer networks with undirected and directed interlayer couplings. Based on these analytical results, explicit relationships between synchronizability and network parameters are established for two distinct synchronization regions. Numerical examples are provided to validate the theoretical results, demonstrating that the intralayer and interlayer coupling strengths, together with the number of layers, jointly determine synchronizability. The main contributions are summarized as follows:

1. Derive exact analytical expressions for the eigenvalues of the supra-Laplacian matrix in multilayer networks with identical intralayer topologies.
2. Establish explicit synchronizability criteria for bounded and unbounded synchronization regions.
3. Reveal the distinct effects of undirected and directed interlayer couplings on network synchronizability.
4. Characterize how coupling strengths and the number of layers jointly influence synchronization behavior under different synchronization regimes.

The remainder of this paper is organized as follows: In Section 2, we introduce the synchronizability criteria and relevant lemmas. In Section 3, we present the multilayer network models and the analytical derivation of the synchronizability criteria. In Section 4, we provide numerical simulations to verify the theoretical results. Finally, in Section 5, we conclude the paper.

2. Synchronizability criteria

In a multilayer network consisting of M layers [34], the dynamics of the k-th node in the α-th layer are governed by the following equation:

$$\frac{dx_k^\alpha}{dt} = f(x_k^\alpha) - \sigma \sum_{g=1}^{N} l_{kg}^\alpha H_1(x_g^\alpha) - \omega \sum_{\beta=1}^{M} d_k^{\alpha\beta} H_2(x_k^\beta), \tag{2.1}$$

where $x_k^\alpha \in \mathcal{R}^n$ represents the state variable of node k in layer α, $1 \le k \le N$, $1 \le \alpha \le M$, and $M \ge 2$. The function $f(\cdot)$ denotes the intrinsic dynamics of node k, which can take the form of a linear system, a stochastic system, or a chaotic system [38, 39]. The intralayer coupling function $H_1(\cdot) : \mathcal{R}^n \to \mathcal{R}^n$, describes interactions between nodes within the same layer. Its associated coupling strength is $\sigma > 0$. Similarly, $H_2(\cdot) : \mathcal{R}^n \to \mathcal{R}^n$ characterizes interlayer interactions between corresponding nodes in different layers, with $\omega > 0$ as the coupling strength. For simplicity, coupling functions $H_1(x_g^\alpha)$ and $H_2(x_k^\beta)$ are assumed to be linear, represented by a constant matrix Γ. The intralayer connectivity is defined as follows: If node k and node g ($k \ne g$) are connected in layer α, then $l_{kg}^\alpha = -1$; otherwise, $l_{kg}^\alpha = 0$. The diagonal elements are given by $l_{kk}^\alpha = -\sum_{g=1,g\ne k}^{N} l_{kg}^\alpha$. The corresponding intralayer Laplacian matrix is then defined as $L_{\text{intra}}^{(\alpha)} = (\sigma l_{kg}^\alpha) \in \mathcal{R}^{N\times N}$, which encodes the structure of layer α. In the same way, the interlayer coupling structure is determined by the adjacency of corresponding nodes across layers. If a node k in layer α connects to its counterpart in layer β, then $d_k^{\alpha\beta} = -1$; otherwise, $d_k^{\alpha\beta} = 0$. The diagonal elements satisfy $d_k^{\alpha\alpha} = -\sum_{\beta=1,\beta\ne\alpha}^{M} d_k^{\alpha\beta}$. This leads to the interlayer Laplacian matrix, expressed as $L_{\text{inter}} = (\omega d_k^{\alpha\beta}) \in \mathcal{R}^{M\times M}$.

Based on the above analysis, Eq (2.1) can be rewritten in matrix form as follows:

$$\dot{x} = F(x) - (\mathcal{L} \otimes \Gamma)x,$$

where the supra-Laplacian matrix of system in Eq (2.1) is $\mathcal{L} = \mathcal{L}_{\text{intra}} + \mathcal{L}_{\text{inter}}$, the symbol $\otimes$ is the Kronecker product, I_N is an identity matrix of dimension N, and

$$x = \begin{pmatrix} x^{(1)} \\ x^{(2)} \\ \vdots \\ x^{(M)} \end{pmatrix}, \quad x^{(\alpha)} = \begin{pmatrix} x_1^{\alpha} \\ x_2^{\alpha} \\ \vdots \\ x_N^{\alpha} \end{pmatrix},$$

$$F(x) = \begin{pmatrix} \tilde{f}(x^{(1)}) \\ \tilde{f}(x^{(2)}) \\ \vdots \\ \tilde{f}(x^{(M)}) \end{pmatrix}, \quad \tilde{f}(x^{(\alpha)}) = \begin{pmatrix} f(x_1^{\alpha}) \\ f(x_2^{\alpha}) \\ \vdots \\ f(x_N^{\alpha}) \end{pmatrix},$$

$$\mathcal{L}_{\text{intra}} = \begin{pmatrix} L_{\text{intra}}^{(1)} & \mathbf{0} & \cdots & \mathbf{0} \\ \mathbf{0} & L_{\text{intra}}^{(2)} & \cdots & \mathbf{0} \\ \vdots & \vdots & \ddots & \vdots \\ \mathbf{0} & \mathbf{0} & \cdots & L_{\text{intra}}^{(M)} \end{pmatrix},$$

and

$$\mathcal{L}_{\text{inter}} = L_{\text{inter}} \otimes I_N.$$

The synchronizability of multilayer networks is characterized by the smallest nonzero eigenvalue Λ_2 and the largest eigenvalue $\Lambda_{\max}$ of the supra-Laplacian matrix $\mathcal{L}$. Depending on the stability interval of the master stability function, the synchronization region can be classified into four types: (1) an unbounded synchronization region, (2) a bounded synchronization region, (3) a synchronization region composed of multiple disjoint bounded and unbounded intervals, and (4) an empty synchronization region. In this study, attention is restricted to the first two cases. For networks with an unbounded synchronization region, a larger value of Λ_2 indicates stronger synchronizability. In contrast, when the synchronization region is bounded, synchronizability is enhanced as the eigenratio $\frac{\Lambda_2}{\Lambda_{\max}}$ increases.

Lemma 2.1 ([40]). If A_{ii} is a square matrix, $i = 1, \ldots, m$, then

$$\begin{vmatrix} A_{11} & A_{12} & \cdots & A_{1m} \\ \mathbf{0} & A_{22} & \cdots & A_{2m} \\ \vdots & \vdots & \ddots & \vdots \\ \mathbf{0} & \mathbf{0} & \cdots & A_{mm} \end{vmatrix} = |A_{11}| \cdot |A_{22}| \cdots |A_{mm}|.$$

3. Exact derivation of synchronizability criteria

In this section, multilayer networks consisting of identical M layers are investigated, in which the interlayer couplings are either undirected or directed, and each node in a given layer is connected to its counterparts in adjacent layers. The detailed structure of the multilayer network model is illustrated in Figure 1. For this configuration, a new analytical approach is required for the computation of the eigenvalues.

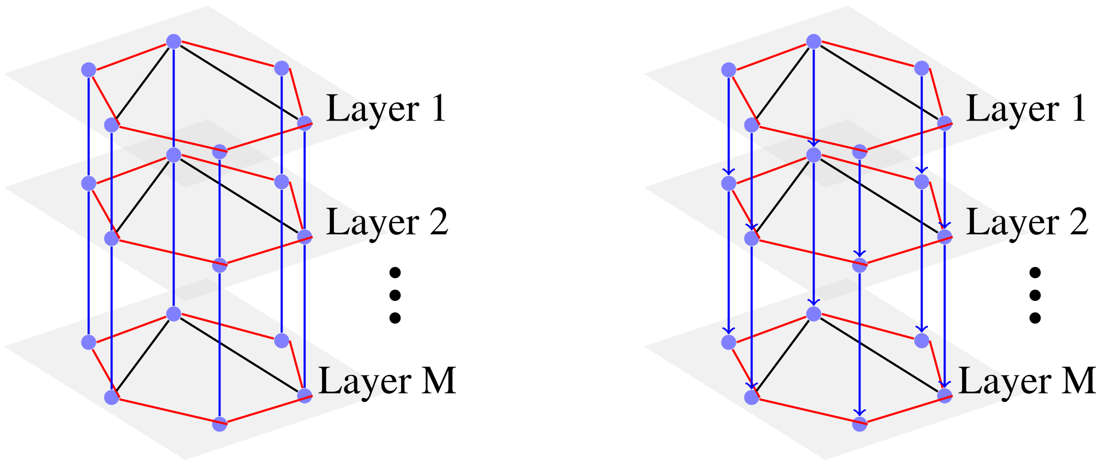

(a) Undirected interlayer coupling (b) Directed interlayer coupling

Figure 1. A detailed illustration of multilayer networks with identical intralayer topologies.

3.1. Synchronizability criteria for undirected multilayer networks

To obtain exact synchronizability criteria, the structure of each layer is assumed to be identical, i.e., $L^{(1)}_{\text{intra}} = L^{(2)}_{\text{intra}} = \cdots = L^{(M)}_{\text{intra}} = L$. The supra-Laplacian matrix for the undirected multilayer networks is given by

$$\mathcal{L}_{\text{undirected}} = \begin{pmatrix} \sigma L + \omega I_N & -\omega I_N & \mathbf{0} & \cdots & \mathbf{0} \\ -\omega I_N & \sigma L + 2\omega I_N & -\omega I_N & \cdots & \mathbf{0} \\ \mathbf{0} & -\omega I_N & \sigma L + 2\omega I_N & \cdots & \mathbf{0} \\ \vdots & \vdots & \vdots & \ddots & \vdots \\ \mathbf{0} & \mathbf{0} & \mathbf{0} & \cdots & \sigma L + \omega I_N \end{pmatrix}.$$

Then, the supra-Laplacian matrix $\mathcal{L}_{\text{undirected}}$ reads as

$$\mathcal{L}_{\text{undirected}} = \sigma I_M \otimes L + \omega T \otimes I_N,$$

where

$$T = \begin{pmatrix} 1 & -1 & 0 & \cdots & 0 \\ -1 & 2 & -1 & \cdots & 0 \\ 0 & -1 & 2 & \cdots & 0 \\ \vdots & \vdots & \vdots & \ddots & \vdots \\ 0 & 0 & 0 & \cdots & 1 \end{pmatrix}_{M\times M}.$$

Suppose that u_i and v_j are the eigenvectors corresponding to the eigenvalues λ_i of L and μ_j of T, respectively, namely,

$$Lu_i = \lambda_i u_i, \quad Tv_j = \mu_j v_j, \quad i = 1, 2, \ldots, N, \quad j = 0, 1, \ldots, M-1.$$

Based on the properties of Kronecker product ($(A \otimes B)(x \otimes y) = (Ax) \otimes (By)$), it follows that

$$(\sigma I_M \otimes L)(v_j \otimes u_i) = \sigma\lambda_i (v_j \otimes u_i),$$

$$(\omega T \otimes I_N)(v_j \otimes u_i) = \omega\mu_j(v_j \otimes u_i).$$

From the expression for $\mathcal{L}_{\text{undirected}} = \sigma I_M \otimes L + \omega T \otimes I_N$, it shows that

$$\mathcal{L}_{\text{undirected}}(v_j \otimes u_i) = (\sigma\lambda_i + \omega\mu_j)(v_j \otimes u_i).$$

To this end, the eigenvalues of $\mathcal{L}_{\text{undirected}}$ are

$$\begin{aligned}\Lambda &= \sigma\lambda_i + \omega\mu_j \\ &= \sigma\lambda_i + 2\omega\Big(1 - \cos\frac{\pi j}{M}\Big), \quad i = 1, 2, \ldots, N, \quad j = 0, 1, \ldots, M-1,\end{aligned}$$

where $\lambda_i (i = 1, 2, \ldots, N)$ are the eigenvalues of matrix L, ordered as $0 = \lambda_1 < \lambda_2 \leq \cdots \leq \lambda_N$, and $\mu_j = 2\big(1 - \cos\frac{\pi j}{M}\big)$, $j = 0, 1, \ldots, M-1$, are the eigenvalues of matrix T.

Comparing the nonzero minimum and maximum eigenvalues of $\mathcal{L}_{\text{undirected}}$ yields

$$\begin{aligned}\Lambda_2 &= \min\Big\{\sigma\lambda_2, 2\omega\Big(1 - \cos\frac{\pi}{M}\Big)\Big\}, \\ \Lambda_{\max} &= \sigma\lambda_N + 2\omega\Big(1 - \cos\frac{(M-1)\pi}{M}\Big).\end{aligned}$$

Finally, the synchronizability criteria are given by

$$\begin{aligned}\Theta_1 &= \min\Big\{\sigma\lambda_2, 2\omega\Big(1 - \cos\frac{\pi}{M}\Big)\Big\}, \\ &= \begin{cases} \Theta_1(I) = \sigma\lambda_2, & \text{Case 1} : \sigma\lambda_2 \leq 2\omega\big(1 - \cos\frac{\pi}{M}\big), \\ \Theta_1(II) = 2\omega\big(1 - \cos\frac{\pi}{M}\big), & \text{Case 2} : \sigma\lambda_2 > 2\omega\big(1 - \cos\frac{\pi}{M}\big), \end{cases}\end{aligned} \tag{3.1}$$

and

$$\begin{aligned}\Phi_1 &= \frac{\min\{\sigma\lambda_2, 2\omega\big(1 - \cos\frac{\pi}{M}\big)\}}{\sigma\lambda_N + 2\omega\big(1 - \cos\frac{(M-1)\pi}{M}\big)} \\ &= \begin{cases} \Phi_1(I) = \frac{\sigma\lambda_2}{\sigma\lambda_N + 2\omega\left(1 - \cos\frac{(M-1)\pi}{M}\right)}, & \text{Case 1}, \\ \Phi_1(II) = \frac{2\omega\left(1 - \cos\frac{\pi}{M}\right)}{\sigma\lambda_N + 2\omega\left(1 - \cos\frac{(M-1)\pi}{M}\right)}, & \text{Case 2}. \end{cases}\end{aligned} \tag{3.2}$$

Table 1 shows the variations of Λ_2 and $\frac{\Lambda_2}{\Lambda_{\max}}$ with respect to the network parameters M, ω, and σ in undirected multilayer networks. Based on these exact results of Eqs (3.1) and (3.2), the corresponding dependence of synchronizability on M, ω, and σ is summarized in Table 2. These parameters have a significant influence on synchronizability: Increasing the number of layers M weakens synchronizability, whereas increasing the coupling strengths ω or σ enhances it.

Table 1. Changes of Λ_2 and $\frac{\Lambda_2}{\Lambda_{\max}}$ regarding M, ω, σ in undirected multilayer networks.

		Increase of M	Increase of ω	Increase of σ
$\min \Lambda_2$	$\Theta_1(I)$	–	–	↑
	$\Theta_1(II)$	↓	↑	–
$\min \frac{\Lambda_2}{\Lambda_{\max}}$	$\Phi_1(I)$	↓	↓	↑
	$\Phi_1(II)$	↓	↑	↓

–: unchanged; ↑: increase; ↓: decrease.

Table 2. Changes of synchronizability regarding M, ω, σ in undirected multilayer networks.

		Unbounded synchronization region	Bounded synchronization region
Increase of M	Case 1	–	↓
	Case 2	↓	↓
Increase of ω	Case 1	–	↓
	Case 2	↑	↑
Increase of σ	Case 1	↑	↑
	Case 2	–	↓

–: unchanged; ↑: increase; ↓: decrease.

3.2. *Synchronizability criteria for directed multilayer networks*

In contrast to the undirected case, a directed multilayer network is introduced by enabling the intra-layer or interlayer couplings to be asymmetric. In such a framework, each layer consists of directed links that encode the directionality of interactions among nodes, while directed interlayer connections describe asymmetric information between corresponding nodes in different layers. As a result, the associated supra-Laplacian matrix becomes asymmetric, and its spectral properties are generally complex-valued, leading to different synchronizability characteristics compared with undirected multilayer networks. To obtain exact results for synchronizability, only directed interlayer couplings are considered in the proposed network model. The supra-Laplacian matrix $\mathcal{L}_{\text{directed}}$ is

$$\mathcal{L}_{\text{directed}} = \begin{pmatrix} \sigma L + \omega I_N & -\omega I_N & \mathbf{0} & \cdots & \mathbf{0} \\ \mathbf{0} & \sigma L + \omega I_N & -\omega I_N & \cdots & \mathbf{0} \\ \mathbf{0} & \mathbf{0} & \sigma L + \omega I_N & \cdots & \mathbf{0} \\ \vdots & \vdots & \vdots & \ddots & \vdots \\ \mathbf{0} & \mathbf{0} & \mathbf{0} & \cdots & \sigma L \end{pmatrix}.$$

By applying the properties of determinant and Lemma 2.1, the characteristic polynomial of $\mathcal{L}_{\text{directed}}$ is derived as follows:

$$\begin{aligned} |\Lambda I_{MN} - \mathcal{L}_{\text{directed}}| &= \begin{vmatrix} (\Lambda-\omega)I_N - \sigma L & \omega I_N & \mathbf{0} & \cdots & \mathbf{0} \\ \mathbf{0} & (\Lambda-\omega)I_N - \sigma L & \omega I_N & \cdots & \mathbf{0} \\ \mathbf{0} & \mathbf{0} & (\Lambda-\omega)I_N - \sigma L & \cdots & \mathbf{0} \\ \vdots & \vdots & \vdots & \ddots & \vdots \\ \mathbf{0} & \mathbf{0} & \mathbf{0} & \cdots & \Lambda I_N - \sigma L \end{vmatrix} \\ &= |(\Lambda-\omega)I_N - \sigma L|^{M-1} |\Lambda I_N - \sigma L|. \end{aligned}$$

It follows that the eigenvalues of $\mathcal{L}_{\text{directed}}$ are given by

$$0, \sigma\lambda_2, \sigma\lambda_3, \ldots, \sigma\lambda_N, \quad \underbrace{\omega}_{M-1}, \quad \underbrace{\sigma\lambda_2 + \omega}_{M-1}, \quad \underbrace{\sigma\lambda_3 + \omega}_{M-1}, \ldots, \underbrace{\sigma\lambda_N + \omega}_{M-1}. \tag{3.3}$$

Based on the results of Eq (3.3), the second smallest and the largest eigenvalues are obtained, that is,

$$\begin{aligned} \Lambda_2 &= \min\{\sigma\lambda_2, \omega\}, \\ \Lambda_{\max} &= \sigma\lambda_N + \omega. \end{aligned}$$

Finally, the synchronizability criteria of directed multilayer networks are

$$\begin{aligned} \Theta_2 &= \min\{\sigma\lambda_2, \omega\}, \\ &= \begin{cases} \Theta_2(III) = \sigma\lambda_2, & \text{Case 3} : \sigma\lambda_2 \leq \omega, \\ \Theta_2(IV) = \omega, & \text{Case 4} : \sigma\lambda_2 > \omega, \end{cases} \end{aligned} \tag{3.4}$$

and

$$\begin{aligned} \Phi_2 &= \frac{\min\{\sigma\lambda_2, \omega\}}{\sigma\lambda_N + \omega} \\ &= \begin{cases} \Phi_2(III) = \frac{\sigma\lambda_2}{\sigma\lambda_N + \omega}, & \text{Case 3}, \\ \Phi_2(IV) = \frac{\omega}{\sigma\lambda_N + \omega}, & \text{Case 4}. \end{cases} \end{aligned} \tag{3.5}$$

Based on the results of Eqs (3.4) and (3.5), the variations of Λ_2 and $\frac{\Lambda_2}{\Lambda_{\max}}$ with respect to parameters M, ω, and σ are summarized in Table 3, and the corresponding synchronizability results are presented in Table 4. In contrast to the undirected case, the number of layers M has no effect on synchronizability in either unbounded or bounded synchronization regions. The influence of the coupling strengths σ and ω is the same as in the undirected case.

Table 3. Changes of Λ_2 and $\frac{\Lambda_2}{\Lambda_{\max}}$ regarding M, ω, σ in directed multilayer networks.

		Increase of M	Increase of ω	Increase of σ
$\min \Lambda_2$	$\Theta_2(III)$	–	–	↑
	$\Theta_2(IV)$	–	↑	–
$\min \frac{\Lambda_2}{\Lambda_{\max}}$	$\Phi_2(III)$	–	↓	↑
	$\Phi_2(IV)$	–	↑	↓

–: unchanged; ↑: increase; ↓: decrease.

Table 4. Changes of synchronizability regarding M, ω, σ in directed multilayer networks.

		Unbounded synchronization region	Bounded synchronization region
Increase of M	Case 3	–	–
	Case 4	–	–
Increase of ω	Case 3	–	↓
	Case 4	↑	↑
Increase of σ	Case 3	↑	↑
	Case 4	–	↓

–: unchanged; ↑: increase; ↓: decrease.

4. Numerical examples

To verify the theoretical synchronizability results summarized in Tables 2 and 4, in this section, we present numerical examples, in which the Erdös–Rényi (ER) network model is adopted as the intralayer network.

4.1. Synchronizability of undirected multilayer networks

The ER network is constructed with connection probability p and total number of nodes N, set to $N = 100$ and $p = 0.1$. Since synchronizability depends on the three parameters M, ω, and σ, only one parameter is varied at a time while the other two are kept fixed.

First, the dependence of synchronizability on the number of layers M is illustrated in Figure 2, with $\omega = 2$ and $\sigma = 1$. In the case of an unbounded synchronization region, Λ_2 initially remains constant and then decreases as M increases. This indicates that the synchronizability of undirected multilayer networks remains unchanged for small values of M and decreases for larger values of M. According to the theoretical result in Eq (3.1), there exists a threshold $M^* = \left[\frac{\pi}{\arccos(1-\frac{\sigma\lambda_2}{2\omega})}\right]$, provided that $\arccos(1 - \frac{\sigma\lambda_2}{2\omega}) > 0$, where $[x]$ is the greatest integer less than or equal to $x > 0$. When the number of layers $M \leq M^*$, $\Theta_1(I) = \sigma\lambda_2$ remains constant. However, for $M > M^*$, Λ_2 is given by $2\omega\left(1 - \cos\frac{\pi}{M}\right)$, which decreases as M increases. For the case of a bounded synchronization region, the eigenratio $\frac{\Lambda_2}{\Lambda_{\max}}$ decreases as M increases, indicating a decline in synchronizability.

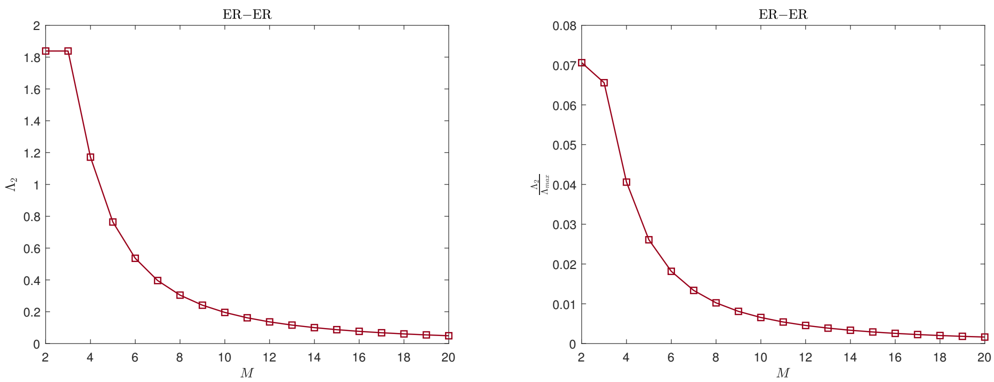

(a) (b)

Figure 2. Distributions of the synchronizability Λ_2 and $\frac{\Lambda_2}{\Lambda_{max}}$ versus the number of layers M, where $\omega = 2, \sigma = 1$. As the number of layers M increases, the synchronizability is weakened.

Second, the dependence of synchronizability on the inter-layer coupling strength ω is illustrated in Figure 3. For the case of an unbounded synchronization region, Λ_2 initially increases with ω and then remains constant. This suggests that the synchronizability is first enhanced and then remains unchanged as ω continues to increase. From a practical perspective, a moderate increase in the inter-layer coupling strength can enhance network synchronizability. For the case of a bounded synchronization region, the eigenratio $\frac{\Lambda_2}{\Lambda_{\max}}$ initially increases with ω but subsequently decreases. This indicates that synchronizability is first enhanced and then weakened as ω continues to increase.

Finally, the dependence of synchronizability on the intra-layer coupling strength σ is illustrated in Figure 4. This case exhibits a trend similar to that observed when varying the inter-layer coupling strength ω. For the case of an unbounded synchronization region, Λ_2 initially increases as σ increases and eventually remains constant. For the bounded synchronization case, synchronizability is initially enhanced but subsequently weakens as the intra-layer coupling strength σ continues to increase.

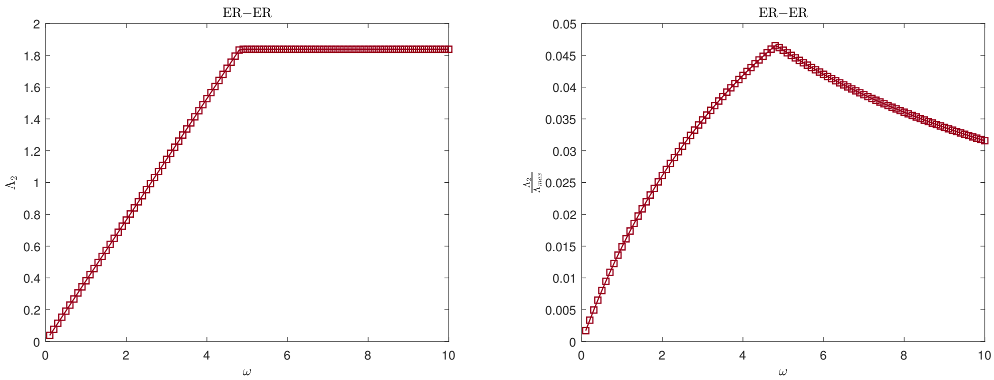

(a) (b)

Figure 3. Distributions of the synchronizability Λ_2 and $\frac{\Lambda_2}{\Lambda_{max}}$ versus the interlayer coupling strength ω, where $M = 5$, $\sigma = 1$. As the interlayer coupling strength ω increases, the synchronizability of networks with an unbounded synchronization region is enhanced and then remains unchanged. For networks with a bounded synchronization region, the synchronizability is first enhanced and then weakened.

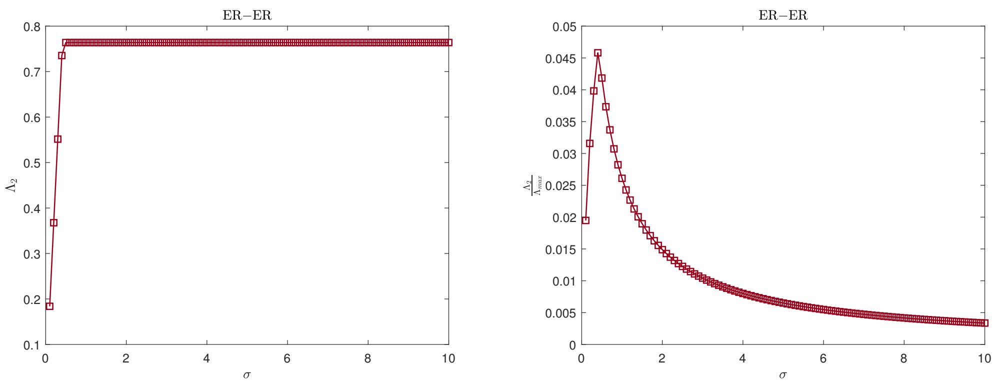

(a) (b)

Figure 4. Distributions of the synchronizability Λ_2 and $\frac{\Lambda_2}{\Lambda_{max}}$ versus the intralayer coupling strength σ, where $M = 5$, $\omega = 2$. The effect of the intralayer coupling strength σ on synchronizability exhibits the same trend as that of the interlayer coupling strength ω.

4.2. Synchronizability of directed multilayer networks

Following the numerical analysis in the previous subsection, the synchronizability of directed multilayer networks is further investigated through numerical simulations. In the same manner, the effects of the individual network parameters M, ω, and σ on synchronizability are examined separately. Figure 5 presents the synchronizability results as a function of M, showing that the trends of Λ_2 and $\frac{\Lambda_2}{\Lambda_{max}}$ remain unchanged, regardless of whether the synchronization region is bounded or unbounded. These numerical results are consistent with the theoretical predictions summarized in Table 4.

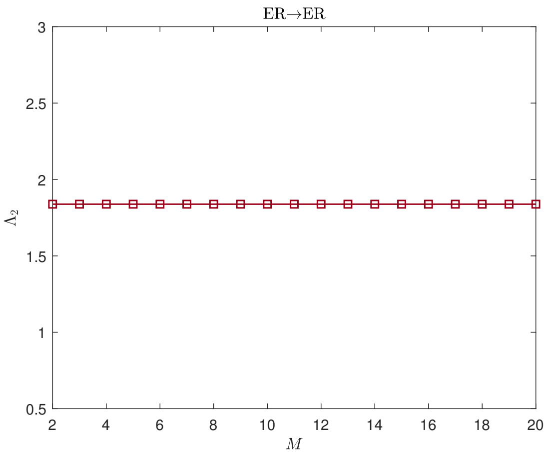

(a)

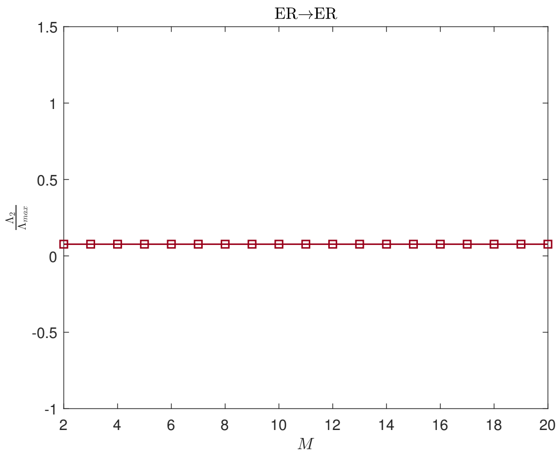

(b)

Figure 5. Distributions of the synchronizability Λ_2 and $\frac{\Lambda_2}{\Lambda_{max}}$ versus the number of layers M, where $\omega = 2$, $\sigma = 1$. Increasing the number of layers does not change the synchronizability.

Figure 6 illustrates the synchronizability of directed multilayer networks as a function of the interlayer coupling strength ω. The variations of Λ_2 and $\frac{\Lambda_2}{\Lambda_{max}}$ in directed networks are the same as those in the undirected case. There exists a threshold interlayer coupling strength, $\omega^* = \sigma\lambda_2$, that determines the synchronizability. Notably, when the synchronization region is bounded, this threshold value ω^* maximizes the highest synchronizability.

In contrast to the effect of the interlayer coupling strength ω, the intralayer coupling strength σ also plays a decisive role in determining network synchronizability, as shown in Figure 7. The overall trend of synchronizability on σ is similar to that on ω, and a threshold value, $\sigma^* = \omega/\lambda_2$, exists at which synchronizability is maximized. A comparison between Figures 6 and 7 further indicates that the interlayer coupling strength has a more pronounced impact on synchronizability than the intralayer coupling strength.

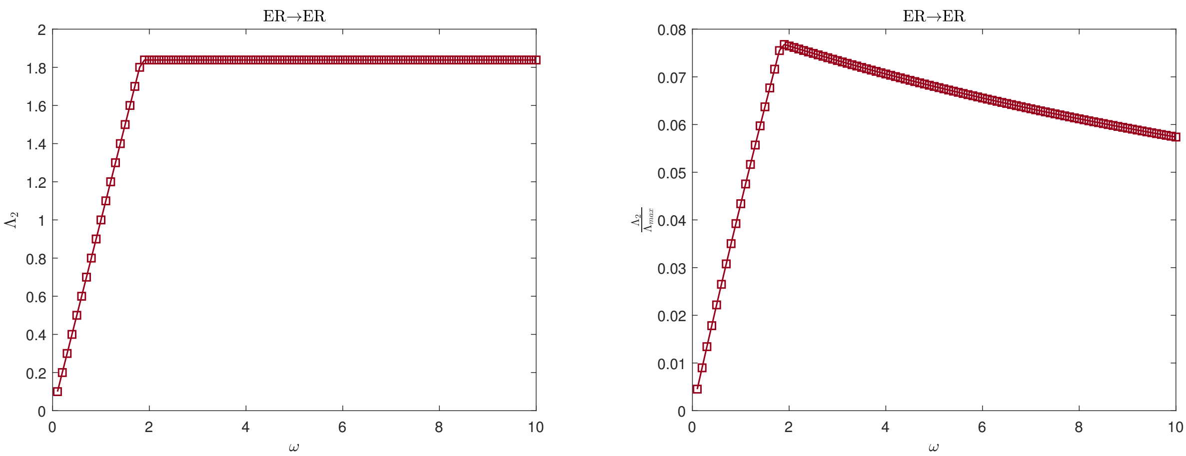

(a) (b)

Figure 6. Distributions of the synchronizability Λ_2 and $\frac{\Lambda_2}{\Lambda_{max}}$ versus the interlayer coupling strength ω, where $M = 5$, $\sigma = 1$. The synchronizability exhibits similar trends under undirected and directed interlayer couplings with respect to ω.

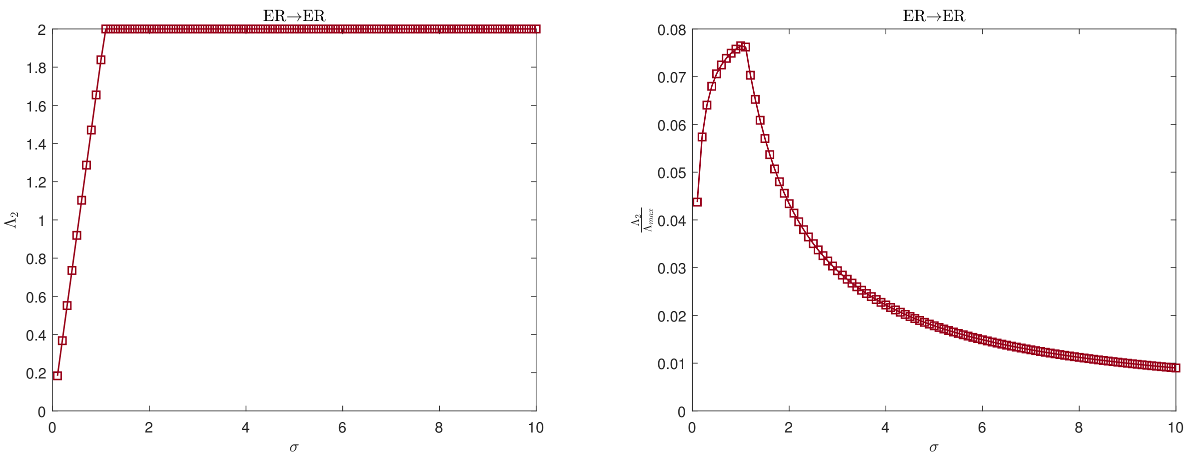

(a) (b)

Figure 7. Distributions of the synchronizability Λ_2 and $\frac{\Lambda_2}{\Lambda_{max}}$ versus the intralayer coupling strength σ, where $M = 5$, $\omega = 2$. The synchronizability exhibits similar trends under undirected and directed interlayer couplings with respect to σ.

4.3. *Phase diagrams of synchronizability for undirected multilayer networks*

In this subsection, we present phase diagrams for synchronizability in a two-dimensional parameter space in Figure 8, with the bounded synchronization region of undirected multilayer networks selected as a representative example. These phase diagrams further validate the theoretical and numerical results.

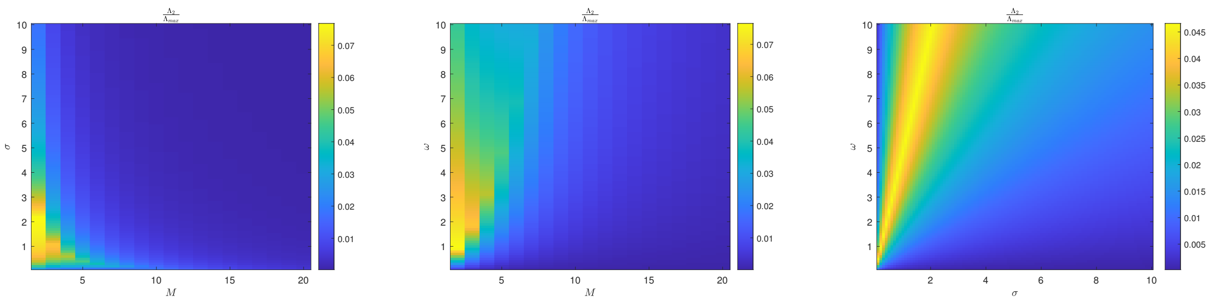

(a) (M, σ) with $\omega = 2, N = 100$ (b) (M, ω) with $\sigma = 1, N = 100$ (c) (σ, ω) with $M = 2, N = 100$

Figure 8. Phase diagrams for synchronizability in a two-dimensional space.

5. Conclusions

In this paper, we investigate the synchronizability of multilayer networks with undirected and directed interlayer couplings. In contrast to other studies on multilayer network synchronizability, the intralayer networks are assumed to be general networks. Based on the structure of the supra-Laplacian matrix, exact expressions for all eigenvalues are derived, and the corresponding relationships governing synchronizability are established. The results demonstrate that the intralayer and interlayer coupling strengths, as well as the number of layers, jointly determine synchronizability, which is further verified through numerical examples. For unbounded and bounded synchronization regions, the variations in the synchronizability criteria exhibit similar trends. In addition, the number of layers plays different roles in synchronizability: Increasing the number of layers weakens synchronizability in undirected networks, whereas it has no effect in directed networks. In particular, the analysis is restricted to multilayer networks with identical intralayer structures and specific interlayer coupling configurations, which are adopted to enable rigorous analytical derivations. More general heterogeneous multilayer topologies and arbitrary directed interlayer couplings may lead to supra-Laplacian matrices whose spectral properties cannot be obtained analytically. Extending this theoretical framework to heterogeneous and more general directed multilayer networks remains an important topic for future research.

Use of AI tools declaration

The authors declare they have not used Artificial Intelligence (AI) tools in the creation of this article.

Conflict of interest

The authors declare there is no conflict of interest.

Acknowledgements

This work was supported by the Scientific Research Fund of Zhejiang Provincial Education Department (No. Y202558907).

Author contributions

Jing Chen: Conceptualization, Methodology, Formal analysis, Investigation, Writing—original draft, Funding acquisition. Dedian Li: Methodology, Formal analysis, Writing—original draft, Programming. Weigang Sun: Supervision, Writing–review and editing. Xinke Zhao: Programming, Validation. All authors have read and agreed to the published version of the manuscript.

References

1. D. Watts, S. Strogatz, Collective dynamics of small-world networks, *Nature*, **393** (1998), 440–442. https://doi.org/10.1038/30918

2. A. Barabási, R. Albert, Emergence of scaling in random networks, *Science*, **286** (1999), 509–512. https://doi.org/10.1126/science.286.5439.509

3. J. Delgado, Emergence of social conventions in complex networks, *Artif. Intell.*, **141** (2002), 171–185. https://doi.org/10.1016/S0004-3702(02)00262-X

4. E. Bullmore, O. Sporns, The economy of brain network organization, *Nat. Rev. Neurosci.*, **13** (2012), 336–349. https://doi.org/10.1038/nrn3214

5. G. A. Pagani, M. Aiello, The power grid as a complex network: A survey, *Phys. A*, **392** (2013), 2688–2700. https://doi.org/10.1016/j.physa.2013.01.023

6. J. X. Chen, J. Q. Hu, R. Kapral, Chemical logic gates on active colloids, *Adv. Sci.*, **11** (2024), 2305695. https://doi.org/10.1002/advs.202305695

7. A. Arenas, A. Díaz-Guilera, J. Kurths, Y. Moreno, C. Zhou, Synchronization in complex networks, *Phys. Rep.*, **469** (2008), 93–153. https://doi.org/10.1016/j.physrep.2008.09.002

8. Z. Wang, Y. Wang, Attack-resilient pulse-coupled synchronization, *IEEE Trans. Control Netw. Syst.*, **6** (2019), 338–351. https://doi.org/10.1109/TCNS.2018.2817922

9. C. Chen, K. Xie, F. L. Lewis, S. Xie, R. Fierro, Adaptive synchronization of multi-agent systems with resilience to communication link faults, *Automatica*, **111** (2020), 108636. https://doi.org/10.1016/j.automatica.2019.108636

10. J. Gómez-Gardenes, Y. Moreno, A. Arenas, Paths to synchronization on complex networks, *Phys. Rev. Lett.*, **98** (2007), 034101. https://doi.org/10.1103/PhysRevLett.98.034101

11. K. Sone, Y. Ashida, T. Sagawa, Topological synchronization of coupled nonlinear oscillators, *Phys. Rev. Res.*, **4** (2022), 023211. https://doi.org/10.1103/PhysRevResearch.4.023211

12. G. R. Chen, Z. S. Duan, Network synchronizability analysis: A graph-theoretic approach, *Chaos*, **18** (2008), 037102. https://doi.org/10.1063/1.2965530

13. F. Della Rossa, P. De Lellis, Synchronization and pinning control of stochastic coevolving networks, *Annu. Rev. Control*, **53** (2022), 147–160. https://doi.org/10.1016/j.arcontrol.2022.04.005

14. R. M. D'Souza, M. Di Bernardo, Y. Y. Liu, Controlling complex networks with complex nodes, *Nat. Rev. Phys.*, **5** (2023), 250–262. https://doi.org/10.1038/s42254-023-00566-3

15. S. Jafarizadeh, D. Veitch, F. Tofigh, J. Lipman, M. Abolhasan, Optimal synchronizability in networks of coupled systems: topological view, *IEEE Trans. Netw. Sci. Eng.*, **8** (2021), 1517–1530. https://doi.org/10.1109/TNSE.2021.3063240

16. J. T. Lizier, F. Bauer, F. M. Atay, J. Jost, Analytic relationship of relative synchronizability to network structure and motifs, *Proc. Natl. Acad. Sci.*, **120** (2023), e2303332120. https://doi.org/10.1073/pnas.2303332120

17. D. Li, W. Sun, Optimizing synchronizability of small-world networks via adjusting edge weights, *J. Complex Netw.*, **13** (2025), cnaf031. https://doi.org/10.1093/comnet/cnaf031

18. J. B. Liu, X. Wang, J. Cao, The coherence and properties analysis of balanced 2^p-ary tree networks, *IEEE Trans. Netw. Sci. Eng.*, **11** (2024), 4719–4728. https://doi.org/10.1109/TNSE.2024.3395710

19. S. Zaman, Spectral analysis of three invariants associated to random walks on rounded networks with $2n$-pentagons, *Int. J. Comput. Math.*, **99** (2022), 465–485. https://doi.org/10.1080/00207160.2021.1919303

20. J. Chen, W. Sun, J. Wang, Topology design for leader-follower coherence in noisy asymmetric networks, *Phys. Scr.*, **98** (2023), 015215. https://doi.org/10.1088/1402-4896/aca9a3

21. X. F. Wang, G. R. Chen, Synchronization in small-world dynamical networks, *Int. J. Bifurcation Chaos*, **12** (2002), 187–192. https://doi.org/10.1142/S0218127402004292

22. M. Barahona, L. M. Pecora, Synchronization in small-world systems, *Phys. Rev. Lett.*, **89** (2002), 054101. https://doi.org/10.1103/PhysRevLett.89.054101

23. X. Zhang, Y. Wu, Synchronizability of multilayer directed dutch windmill networks, *Fractal Fract.*, **6** (2022), 537. https://doi.org/10.3390/fractalfract6100537

24. A. Sole-Ribalta, M. De Domenico, N. E. Kouvaris, A. Diaz-Guilera, S. Gomez, A. Arenas, Spectral properties of the Laplacian of multiplex networks, *Phys. Rev. E*, **88** (2013), 032807. https://doi.org/10.1103/PhysRevE.88.032807

25. S. Boccaletti, G. Bianconi, R. Criado, C. I. DelGenio, J. Gómez-Gardeñes, M. Romance, et al., The structure and dynamics of multilayer networks, *Phys. Rep.*, **544** (2014), 1–122. https://doi.org/10.1016/j.physrep.2014.07.001

26. S. Majhi, S. Ghosh, P. K. Pal, S. Pal, T. K. Pal, D. Ghosh, et al., Patterns of neuronal synchrony in higher-order networks, *Phys. Life Rev.*, **52** (2025), 144–170. https://doi.org/10.1016/j.plrev.2024.12.013

27. J. Zhuang, J. Cao, L. Tang, Y. Xia, M. Perc, Synchronization analysis for stochastic delayed multilayer network with additive couplings, *IEEE Trans. Syst. Man Cybern. Syst.*, **50** (2020), 4807–4816. https://doi.org/10.1109/TSMC.2018.2866704

28. P. K. Pal, M. S. Anwar, M. Perc, D. Ghosh, Global synchronization in generalized multilayer higher-order networks, *Phys. Rev. Res.*, **6** (2024), 033003. https://doi.org/10.1103/PhysRevResearch.6.033003

29. X. Wu, X. Wu, C. Y. Wang, B. Mao, J. A. Lu, J. Lü, et al., Synchronization in multiplex networks, *Phys. Rep.*, **1060** (2024), 1–54. https://doi.org/10.1016/j.physrep.2024.01.005

30. H. Liu, J. Xu, Z. Li, X. Wang, J. Lü, Z. Zeng, Optimizing synchronizability of multilayer networks based on the graph comparison method, *IEEE Trans. Circuits Syst. I: Regular Papers*, **67** (2020), 1740–1751. https://doi.org/10.1109/TCSI.2019.2963687

31. X. Wei, X. Wu, J. A. Lu, J. Wei, J. Zhao, Y. Wang, Synchronizability of two-layer correlation networks, *Chaos*, **31** (2021), 103124. https://doi.org/10.1063/5.0056482

32. X. Li, Y. Wu, Synchronizability of multilayer totally homogeneous networks, *Mod. Phys. Lett. B*, **39** (2025), 2450478. https://doi.org/10.1142/S0217984924504785

33. L. Tang, X. Wu, J. Lü, J. A. Lu, R. M. D'Souza, Master stability functions for complete, intralayer, and interlayer synchronization in multiplex networks of coupled Rössler oscillators, *Phys. Rev. E*, **99** (2019), 012304. https://doi.org/10.1103/PhysRevE.99.012304

34. L. Zhang, Y. Wu, Synchronizability of multilayer networks with K-nearest-neighbor topologies, *Front. Phys.*, **8** (2020), 571507. https://doi.org/10.3389/fphy.2020.571507

35. M. M. Xu, J. A. Lu, J. Zhou, Synchronizability and eigenvalues of two-layer star networks, *Acta Phys. Sin.*, **65** (2016), 028902. https://doi.org/10.7498/aps.65.028902

36. J. Li, Y. Luan, X. Wu, J. A. Lu, Synchronizability of double-layer dumbbell networks, *Chaos*, **31** (2021), 073101. https://doi.org/10.1063/5.0049281

37. J. Hu, Y. Peng, X. Wu, Optimal inter-layer connections for maximizing synchronizability in two-layer chain network, *Chaos*, **35** (2025), 083127. https://doi.org/10.1063/5.0279141

38. A. Amirkhani, A. H. Barshooi, Consensus in multi-agent systems: A review, *Artif. Intell. Rev.*, **55** (2022), 3897–3935. https://doi.org/10.1007/s10462-021-10097-x

39. Y. Zhang, P. Lin, J. Chen, W. Sun, A hybrid cryptosystem for medical image security: Integrating finite fields with conservative hyperchaos, *Nonlinear Dyn.*, **114** (2026), 129. https://doi.org/10.1007/s11071-025-11994-4

40. R. Bhatia, *Matrix Analysis*, Springer, New York, 1997. https://doi.org/10.1007/978-1-4612-0653-8

AIMS Press